Theory of anisotropic superexchange in insulating cuprates

N. E. Bonesteel
Theoretische Physik, Eidgenössische Technische Hochschule-Hönggerberg, CH-8093 Zürich, Switzerland
(Received 22 June 1992; revised manuscript received 25 February 1993)

Spin-orbit corrections to superexchange are calculated using the method of Moriya [T. Moriya, Phys. Rev. **120**, 91 (1960)] for two of the insulating parent compounds of the cuprate superconductors: (1) $La_{2-x}Nd_xCuO_4$ where the CuO_6 octahedra forming each CuO layer are tilted in staggered fashion about an axis which depends on x and temperature and (2) $YBa_2Cu_3O_{6+x}$ ($x \lesssim 0.4$) where the CuO layers form CuO_2-Y-CuO_2 bilayers in which the in-plane O^{2-} ions are displaced uniformly toward the Y^{3+} layer. For (1) a simple formula is derived for the weak ferromagnetic moment in each CuO layer as a function of the tilting axis and magnitude. For (2) it is shown that the anisotropic corrections to superexchange are different from what has previously been assumed. For the correct spin Hamiltonian a classical Néel state in which the Cu spins are lying in the plane is unstable in a single CuO layer, but when a bilayer is considered there is a critical value of the interlayer exchange coupling which stabilizes this state. For both cases (1) and (2) spin-wave spectra are calculated and shown to compare favorably with experiment.

I. INTRODUCTION

Spin-orbit (SO) coupling causes electron spins to precess as they move through the electric field of a crystal lattice. Within the tight-binding approximation this precession appears as a small spin rotation which occurs whenever an electron tunnels between two Wannier orbitals. As first shown by Moriya[1] this rotation can have important consequences in antiferromagnetic (AFM) Mott insulators; when it is included in Anderson's calculation[2] of superexchange then anisotropic corrections to the otherwise isotropic effective spin Hamiltonian are generated. These corrections, known as Dzyaloshinski-Moriya (DM) interactions[1,3,4], lift any ground-state degeneracy associated with rotational invariance in spin space and are responsible for such effects as weak ferromagnetism and the existence of spin-wave anisotropy gaps.

The subject of this paper is the DM interactions which exist in the distorted CuO layers of the insulating AFM parent phases of the cuprate superconductors. We will be concerned both with the microscopic origin of these interactions and their physical consequences. Probably the best known example of the effects of DM interactions in the cuprates occurs in La_2CuO_4.[5] In this material a structural phase transition occurs from a high-temperature tetragonal (HTT) phase (space group $I4/mmm$) to a low-temperature orthorhombic (LTO) phase (space group $Bmab$). In the LTO phase the CuO_6 octahedra forming each CuO layer tilt in a staggered pattern about the $\langle 110 \rangle$ axis and this distortion results in DM interactions which induce a weak ferromagnetic moment in each layer.[5] Another example of the effects of DM interactions in the cuprates is the easy-plane anisotropy which has been observed in the spin-wave spectrum of the AFM insulating phase of $YBa_2Cu_3O_{6+x}$ ($x \lesssim 0.4$).[6] In this case the relevant structural feature is that the CuO layers form CuO_2-Y-CuO_2 bilayers in which the negatively charged in-plane O^{2-} ions are uniformly buckled towards the positively charged Y^{3+} layer.

One motivation for the present work is that in a recent paper[7] a "one-band" description of SO coupling in both insulating and doped La_2CuO_4 in the presence of various tilting distortions was studied using the Hamiltonian

$$H_{\text{flux}} = -t \sum_{\substack{\langle ij \rangle \\ \alpha}} \left\{ e^{i\phi_{ij}\alpha} c^\dagger_{i\alpha} c_{j\alpha} + \text{H.c.} \right\} + U \sum_i n_{i\uparrow} n_{i\downarrow}. \tag{1.1}$$

Here $c^\dagger_{i\alpha}$ creates an electron with spin α at site i, $n_{i\alpha}$ is the corresponding number operator, $\phi_{i,i+\hat{\mathbf{x}}} \simeq (-1)^{(x_i+y_i)} 0.1\theta$, $\phi_{i,i+\hat{\mathbf{y}}} = -\phi_{i,i+\hat{\mathbf{x}}}$ where θ is the octahedral tilt angle, and in the exponent $\alpha = +\frac{1}{2}$ ($\alpha = -\frac{1}{2}$) for up (down) spins. The x and y components of site i are denoted x_i and y_i, and $\hat{\mathbf{x}}$ and $\hat{\mathbf{y}}$ are unit vectors. Hamiltonian (1.1) describes a correlated tight-binding band of electrons which move in a background of staggered flux where up and down spin electrons have opposite charge. This flux is simply the Berry's phase associated with spin precession about the z axis in spin space. In Ref. 7 the effective Hamiltonian describing the large U/t limit of (1.1) was derived and at half-filling the classical spin ground state was found to have no weak ferromagnetic moment. It is shown here that this result is not in conflict with the experimental observation of such a moment in the LTO phase of La_2CuO_4. Hamiltonian (1.1) is a correct description of electrons in a tilt-distorted CuO layer when the system is viewed in the appropriate *site-dependent coordinate system in spin space.* When local rotations are performed to transform the system back to the physical spin-space coordinate system a weak ferromagnetic moment which agrees with experiment appears.

A similar approach to weak ferromagnetism has been

discussed recently by Shekhtman, Entin-Wohlman, and Aharony (SEA) (Ref. 8) who also studied the DM interactions induced by tilting distortions in La_2CuO_4. SEA were able to show that, quite generally, the DM interactions present on a single Cu-O-Cu bond are isotropic when the bond is viewed in the appropriate local coordinate system in spin space. This observation led them to the interesting conclusion that any physical anisotropy (i.e., anisotropy which cannot be "gauged away" by local rotations) must arise from the *frustration* of these bonds. By applying this idea to the LTO phase of La_2CuO_4 SEA were able to successfully account for the observed weak ferromagnetism in this material. In this paper we calculate the DM interactions which occur in the presence of tilting distortions in which the CuO_6 octahedra can tilt about any axis, not just $\langle 110 \rangle$. Such general tilting distortions may have physical relevance because they describe at least the average structure of $La_{2-x}Nd_xCuO_4$ when $x \lesssim 0.5$.[9,10] The main result of our analysis is that regardless of the octahedral tilt axis the effective Hamiltonian describing a single layer can always be transformed into (1.1), to lowest order in θ. However, the coordinate system in spin space in which (1.1) holds changes as the tilt axis changes so that the ratio of the weak ferromagnetic moment to the size of the tilting distortion depends on the tilt axis in a simple way which we derive in Sec. IV. These results provide a potential experimental test of the "anisotropy through frustration" idea of SEA (Ref. 8) and justifies the use of (1.1) in Ref. 7.

A second motivation for this work is the puzzling observation by Coffey, Rice, and Zhang[11] that the DM interactions in a single buckled CuO layer of $YBa_2Cu_3O_{6+x}$ tend to stabilize an incommensurate spiral spin configuration, while neutron-scattering experiments see no sign of such a spiral.[6] It is shown here that if an effective spin Hamiltonian for a single CuO layer in $YBa_2Cu_3O_{6+x}$ is derived using the same method as for $La_{2-x}Nd_xCuO_4$ then a classical Néel state with spins lying in the xy plane is indeed unstable; complex frequencies corresponding to exponentially growing unstable modes appear in the classical linearized spin-wave spectrum. However, when instead of a *single* CuO layer a CuO_2-Y-CuO_2 *bilayer* is considered these complex frequencies disappear for a critical value of the interlayer coupling $J_{12}^c \sim 10^{-3}J$, well below the lower limit on J_{12} set by experiment,[6] and the Néel state becomes stable. This stabilization occurs because the DM interactions in the upper and lower planes favor spirals with opposite senses (a consequence of the inversion symmetry of the $YBa_2Cu_3O_{6+x}$ unit cell) and this spiraling is frustrated by the interlayer coupling. We also find that when J_{12} is large enough not only does the Néel state become stable, but the spin-wave spectrum shows an in-plane gapless mode and an out-of-plane gapped mode in agreement with experiment.[6] This result shows that the "easy-plane" anisotropy in $YBa_2Cu_3O_{6+x}$, in fact, arises from frustration of DM interactions in accordance with the general principle of SEA.[8]

This paper is organized as follows. In Sec. II the structural and magnetic properties of $La_{2-x}Nd_xCuO_4$ and $YBa_2Cu_3O_{6+x}$ which are relevant for this paper are discussed. The SO modification of superexchange due to the structural distortions in these materials is calculated in Sec. III and the resulting classical ground-state and spin-wave excitation spectra for $La_{2-x}Nd_xCuO_4$ and $YBa_2Cu_3O_{6+x}$ are presented in Secs. IV and V, respectively. Finally, Sec. VI summarizes the conclusions of the paper.

II. RELEVANT EXPERIMENTAL FACTS

A. $La_{2-x}Nd_xCuO_4$

The $La_{2-x}Nd_xCuO_4$ system shows a rich structural phase diagram as a function of x and temperature. As mentioned above when $x = 0$ the material undergoes a phase transition from the HTT phase to the LTO phase. It is also known that when enough Nd is doped into the system ($x > 0.5$) the material crystallizes into the T' structure of pure Nd_2CuO_4.[12] However, for smaller Nd concentration ($x \lesssim 0.4$) there is still a HTT $\rightarrow$ LTO transition, and as the temperature is lowered further there is a second transition into a structural phase with space group *Pccn*.[9,10] In both the LTO and *Pccn* phases the CuO_6 octahedra forming each CuO layer tilt in a staggered fashion through an angle $\theta(\simeq 0.05)$ about first the $(\cos\chi, \sin\chi, 0)$ and then the $(\sin\chi, \cos\chi, 0)$ axis in successive CuO layers where $\chi = \pi/4$ in the LTO phase and $0 < \chi < \pi/4$ in the *Pccn* phase. The case $\chi = 0$ corresponds to the low-temperature tetragonal (LTT) phase (space group $P4_2/ncm$) which occurs, for example, in the doped material $La_{1.88}Ba_{0.12}CuO_4$.[13]

Neutron-scattering measurements of the spin structure factor of insulating La_2CuO_4 and subsequent theoretical analysis have shown fairly conclusively that the spin degrees of freedom in this material are well described by an AFM Heisenberg model with exchange coupling $J \simeq 130$ meV.[14] Although this model is adequate for describing most properties of La_2CuO_4 slight deviations from perfect isotropy have been observed experimentally. In particular (i) Thio *et al.*[5] found a first-order weak-ferromagnetic transition as a function of applied magnetic field perpendicular to the CuO planes; and (ii) both neutron-scattering[16] and AFM resonance measurements[17] have shown that the zone-center spin waves in La_2CuO_4 are gapped with an in-plane gap of $\sim$ 1.5 meV and an out-of-plane gap of $\sim$ 2.5 meV. It was immediately realized by the groups which performed these measurements that these effects were manifestations of DM interactions. These interactions have since been calculated microscopically.[8,11,18] The resulting spin Hamiltonian has an Ising-like anisotropy, which is responsible for the zone-center spin-wave gaps, and a ground state in which the spins lie nearly along the orthorhombic c axis except for a slight cant out of the CuO plane which gives each layer a weak ferromagnetic moment. The canting angle is roughly $\Theta_{wf} \sim 0.005$ and so the weak ferromagnetic moment is $\sim 0.003\mu_B$ per Cu site.[5]

B. $YBa_2Cu_3O_{6+x}$

For $x \lesssim 0.4$ the $YBa_2Cu_3O_{6+x}$ system is tetragonal and AFM with the added oxygens going into the chains

presumably at random. When $x \gtrsim 0.4$ the O ions partially order and this leads to a tetragonal $\rightarrow$ orthorhombic transition. At the same doping the planes become metallic and the material becomes a superconductor. Here we are primarily concerned with the tetragonal insulating AFM phase. The key structural feature in this material is that the CuO layers are not equally spaced as they are in the La system but instead form CuO_2-Y-CuO_2 bilayers. The planes forming these bilayers are buckled with the in-plane negatively charged O^{2-} ions displaced uniformly towards the positively charged Y^{3+} layer. The size of the O dispacement out of the plane depends only weakly on x and is roughly 0.22 Å (Ref. 19) and so the Cu-O bonds make an angle of $\theta \simeq 0.1$ with the CuO plane.[19]

Previously the magnetic structure of $YBa_2Cu_3O_{6+x}$ has been modeled assuming each bilayer can be described by a Hamiltonian of the form[20]

$$H = \sum_{a=1,2} \sum_{i,j} \{J_z S^z_{a,i} S^z_{a,j} + J_{xy}(S^x_{a,i} S^x_{a,j} + S^y_{a,i} S^y_{a,j})\} + J_{12} \sum_i \vec{S}_{1,i} \cdot \vec{S}_{2,i} \quad (2.1)$$

The spin-wave spectrum of (2.1) has four branches: a gapless in-plane mode; a gapped out-of-plane mode with of $4S\sqrt{2(J_{xy} - J)J}$; and two high-energy branches with gaps of $4\sqrt{2}S\sqrt{JJ_{12}}$. Neutron scattering has shown the existence of a gapless in-plane mode with spin-wave velocity $\sim$1.0 eV Å ($J \simeq 150$ meV) and a gapped out-of-plane mode with gap ~ 4 meV (Ref. 6) and so the low-energy spectrum of (2.1) agrees with the experiment. At the same time the high-energy modes have not been observed for energy transfers up to 50 meV putting a lower limit on the interlayer coupling of $J_{12} \gtrsim 10^{-2} J$.[6,21] In Sec. V we will show that when the same methods which have been used successfully to describe La_2CuO_4 are applied to $YBa_2Cu_3O_{6+x}$ the resulting spin Hamiltonian is different than (2.1). Nonetheless, it is possible to reproduce the experimentally observed spin-wave spectrum using the new Hamiltonian.

III. SPIN-ORBIT CORRECTIONS TO SUPEREXCHANGE

Superexchange occurs when two magnetic ions interact through their mutual overlap with an intermediate diamagnetic ion.[2] Recently SEA (Ref. 8) have used Moriya's method[1] to derive a fairly general expression for the anisotropic corrections to superexchange due to SO coupling on a single such bond for spin 1/2. Their result, which corrects some omissions in an earlier calculation,[11] has the interesting property that it can be related to an isotropic interaction by a unitary transformation.[8] A similar expression for the anisotropic superexchange on a single bond was implicit[7] and in this section its derivation is sketched to show that in fact the expressions in (Refs. 7 and 8) are the same and to establish notation for the rest of the paper.

In the presence of SO coupling a single Cu-O-Cu bond is described by the Hamiltonian[1,11,8,18]

$$H_{\mathrm{CuOCu}} = \sum_{\alpha,\beta} \Big\{ d^\dagger_{1\alpha}(t_{pd}\delta_{\alpha\beta} + i\vec{\lambda}_1 \cdot \vec{\sigma}_{\alpha\beta}) p_\beta + d^\dagger_{2\alpha}(t_{pd}\delta_{\alpha\beta} + i\vec{\lambda}_2 \cdot \vec{\sigma}_{\alpha\beta}) d_\beta + \mathrm{H.c.} \Big\} + U_{dd}(n_{d1\uparrow} n_{d1\downarrow} + n_{d2\uparrow} n_{d2\downarrow}) + \Delta_{dp} \sum_\alpha p^\dagger_\alpha p_\alpha. \quad (3.1)$$

In the vacuum state for (3.1) the Cu $3d$ and O $2p$ shells are full. The operators $d^\dagger_{i\alpha}$ and $p^\dagger_\alpha$ then create holes with spin α at Cu site i and the O σ orbital, respectively. The (hole) energy splitting between Cu and O sites is Δ_{pd}, the on-site correlation on the Cu is U_{dd}, and t_{pd}, $\vec{\lambda}_1$ and $\vec{\lambda}_2$ are hopping integrals, the latter two resulting from SO coupling.[8,1]

The problem of deriving the effective spin Hamiltonian for (3.1) simplifies upon applying the unitary transformation

$$d'^\dagger_{1\beta} = \sum_\alpha \left\{ \exp\left[i \tan^{-1}\left(\frac{|\vec{\lambda}_1|}{t_{pd}} \right) \frac{\vec{\lambda}_1 \cdot \vec{\sigma}}{|\vec{\lambda}_1|} \right] \right\}_{\alpha\beta} d^\dagger_{1\alpha}, \quad (3.2)$$

$$d'^\dagger_{2\beta} = \sum_\alpha \left\{ \exp\left[i \tan^{-1}\left(\frac{|\vec{\lambda}_2|}{t_{pd}} \right) \frac{\vec{\lambda}_2 \cdot \vec{\sigma}}{|\vec{\lambda}_2|} \right] \right\}_{\alpha\beta} d^\dagger_{2\alpha}. \quad (3.3)$$

When (3.1) is expressed in terms of the primed operators the result is

$$H_{\mathrm{CuOCu}} = \sum_\alpha \left\{ \tilde{t}_{pd} d'^\dagger_{1\alpha} p_\alpha + \tilde{t}_{pd} d'^\dagger_{2\alpha} p_\alpha + \mathrm{H.c.} \right\} + U(n_{1\uparrow} n_{1\downarrow} + n_{2\uparrow} n_{2\downarrow}) + \Delta \sum_\alpha p^\dagger_\alpha p_\alpha, \quad (3.4)$$

where $\tilde{t}_{pd} = (t^2_{pd} + \lambda^2)^{1/2}$ (we will consider only the case where $|\vec{\lambda}_1| = |\vec{\lambda}_2| = \lambda$). The transformation [(3.2) and (3.3)] absorbs the spin precession induced by SO coupling into a redefinition of the local coordinate system in spin space. Such a transformation is possible because the bond is essentially one dimensional; i.e., there are no closed loops around which an electron can hop and acquire a finite spin precession which cannot be transformed away.

The effective spin Hamiltonian resulting from (3.1) in the limit $\tilde{t}_{pd} \gg U_{dd}, \Delta_{pd}$ can now be found using standard methods.[22] The result is $H_{\mathrm{Bond}} = J\vec{S}'_1 \cdot \vec{S}'_2$, with

$$J = \frac{4\tilde{t}^4_{dp}}{\Delta^2_{dp}} \left\{ \frac{1}{\Delta_{dp}} + \frac{1}{U_{dd}} \right\} \quad (3.5)$$

and $\vec{S}'_1 = (1/2) d'^\dagger_{1\alpha} \vec{\sigma}_{\alpha\beta} d'_{1\beta} + O(t/[\Delta_{pd}, U])$. When the unitary transformation [(3.2) and (3.3)] is undone the final result is

$$H_{\mathrm{Bond}} = J\Big[S^z_1 S^z_2 + \cos\phi(S^x_1 S^x_2 + S^y_1 S^y_2) + \sin\phi(S^x_1 S^y_2 - S^y_1 S^x_2) \Big], \quad (3.6)$$

where $\phi \simeq 2|\vec{\lambda}_1 - \vec{\lambda}_2|/t_{pd}$ is the angle through which an electron spin precesses when it hops from site 1 through the intermediate orbital to site 2, and where the z axis in

spin space has been chosen to be parallel to the precession axis $\vec{\lambda}_1 - \vec{\lambda}_2$.

After some algebra it is possible to show that (3.6) is equivalent to the result obtained by SEA.[8] Hamiltonian (3.6) was also derived in precisely the form given above in (Ref. 7) but starting from a one-band description in which the O ions were not included explicitly. The equivalence between the one-band and three-band pictures at half-filling is easy to understand. If the Hamiltonian for a single bond is given by

$$H_{1-\text{band}} = \sum_{\alpha} \left\{ c^{\dagger}_{1\alpha}(-t\delta_{\alpha\beta} + i\vec{\lambda}_{12}\cdot\vec{\sigma}_{\alpha\beta})c^{\dagger}_{2\alpha} + \text{H.c.} \right\} + U\left(n_{1\uparrow}n_{1\downarrow} + n_{2\uparrow}n_{2\downarrow}\right), \tag{3.7}$$

and if for a given t we choose U so that $4(t^2+\lambda_{12}^2)/U = J$ and $\vec{\lambda}_{12} \simeq (t/t_{pd})(\vec{\lambda}_1 - \vec{\lambda}_2)$, then similar arguments to those given above yield (3.6) when $U \gg t$. In what follows we will adopt this one-band approach and describe a given CuO layer with a Hamiltonian of the form

$$H = \sum_{\substack{\langle ij\rangle \\ \alpha,\beta}} \left\{ c^{\dagger}_{i\alpha}\left(-t\delta_{\alpha\beta} + i\vec{\lambda}_{ij}\cdot\vec{\sigma}_{\alpha\beta}\right)c_{\beta} + \text{H.c.} \right\} + U\sum_{i} n_{i\uparrow}n_{i\downarrow}. \tag{3.8}$$

At half-filling there exists an entire class of models with different t, U, and $\vec{\lambda}_{ij}$ values which yield the same effective spin Hamiltonian in the large U/t limit. Away from half-filling this is no longer the case and it is necessary to perform a mapping from the full three-band model to an effective one-band model in order to find the appropriate parameters. In what follows we are only concerned with the half-filled case and so for simplicity we take $t = t_{pd}$.

It remains to compute the $\vec{\lambda}_{ij}$ vectors. At half-filling each Cu ion in a CuO layer has one hole in its $3d$ shell which, in the absence of SO coupling, occupies the $d_{x^2-y^2}$ orbital. If on each Cu site a SO interaction

$$H_{\text{SO}} = \beta\sum_{i}\vec{L}_i\cdot\vec{S}_i \tag{3.9}$$

is included where $\vec{L}_i$ and $\vec{S}_i$ are the orbital angular momentum and the hole spin at site i, respectively, and $\beta \simeq 0.1$ eV for Cu,[23] then higher crystal-field levels – d_{xy}, d_{xz}, and d_{yz} – are mixed into the lowest-lying $d_{x^2-y^2}$ state. These admixtures then modify the hopping integrals and give rise to the $\vec{\lambda}$ terms in (3.1). Moriya[1] derived an expression in second-order perturbation theory for the $\vec{\lambda}_{ij}$ vectors in (3.8) which for our purposes reads

$$\vec{\lambda}_{ij} \simeq \vec{\lambda}_i - \vec{\lambda}_j \simeq \frac{i\beta}{2}\sum_{m}\left\{ \frac{\langle m,i|\vec{L}_i|0,i\rangle}{\epsilon_m - \epsilon_0}t_{ij}(m,\sigma) - \frac{\langle m,j|\vec{L}_j|0,j\rangle^*}{\epsilon_m - \epsilon_0}t_{ji}(m,\sigma)\right\}, \tag{3.10}$$

where $|m,i\rangle$ is a crystal-field split level in the absence of SO coupling labeled by m at site i with $m = 0$ corresponding to $d_{x^2-y^2}$. The energy of the mth level is ϵ_m, and $t_{ij}(m,\sigma)$ is the hopping matrix element in the absence of SO coupling between the Cu orbital m at site i and the O σ orbital between sites i and j. The relevant matrix elements of $\vec{L}$ are

$$\langle x^2-y^2, j|\vec{L}_j|xz,j\rangle = i\hat{\mathbf{y}}, \qquad \langle x^2-y^2, j|\vec{L}_j|yz,j\rangle = -i\hat{\mathbf{x}}, \tag{3.11}$$

and so to evaluate (3.10) only the matrix elements $t_{ij}(m,\sigma)$ need to be determined. This is done below for $La_{2-x}Nd_xCuO_4$ and $YBa_2Cu_3O_{6+x}$.

A. $La_{2-x}Nd_xCuO_4$

In the LTO and *Pccn* phases of $La_{2-x}Nd_xCuO_4$ the CuO_6 octahedra forming a given CuO layer are rotated through an angle $(-1)^{(x_i+y_i)}\theta$ about the axis $(\cos\chi, \sin\chi, 0)$. In general, there are then two CuO bond angles: $\pm\theta\sin\chi$ and $\pm\theta\cos\chi$ for bonds pointing in the x and y directions, respectively. Figure 1(a) shows the Cu xz orbitals and O σ orbital in a typical bond in $La_{2-x}Nd_xCuO_4$. For this bond the hopping from the rotated xz orbitals to the σ orbital is, for small θ,

$$t_{i,i+\hat{\mathbf{x}}}(xz,\sigma) \simeq (-1)^{x_i+y_i}V_{pd\pi}\theta\sin\chi, \qquad t_{i,i+\hat{\mathbf{x}}}(yz,\sigma) \simeq 0, \tag{3.12}$$

and similarly

$$t_{i,i+\hat{\mathbf{y}}}(xz,\sigma) \simeq 0, \qquad t_{i,i+\hat{\mathbf{y}}}(yz,\sigma) \simeq -(-1)^{x_i+y_i}V_{pd\pi}\theta\cos\chi, \tag{3.13}$$

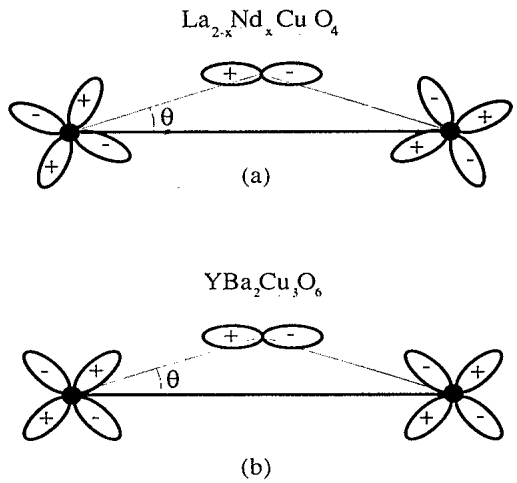

FIG. 1. Cu xz orbitals and O σ orbital in a Cu-O-Cu bond parallel to the x direction in the presence of (a) a tilting distortion ($La_{2-x}Nd_xCuO_4$) and (b) a buckling distortion ($YBa_2Cu_3O_{6+x}$). In (a) the xz orbitals are tilted with respect to the CuO plane while in (b) they are not. As a result, the ratio of the Cu-O bond angle to $t(xy,\sigma)$ (the hopping amplitude between the xy and σ orbitals) is larger in $YBa_2Cu_3O_{6+x}$ than in $La_{2-x}Nd_xCuO_4$.

where $V_{pd\pi}$ is the hopping amplitude between a Cu d_{xy} orbital and an O π_y orbital. The resulting $\vec{\lambda}$ vectors are then

$$\vec{\lambda}_{i,i+\hat{x}} \simeq (-1)^{x_i+y_i}(\lambda_1 \cos\chi, \lambda_2 \sin\chi, 0),$$
$$\vec{\lambda}_{i,i+\hat{y}} \simeq -(-1)^{x_i+y_i}(\lambda_2 \cos\chi, \lambda_1 \sin\chi, 0), \tag{3.14}$$

where

$$\lambda_1 \simeq 0, \tag{3.15}$$

$$\lambda_2 \simeq \frac{V_{pd\pi}\beta}{\epsilon_{xz} - \epsilon_{x^2-y^2}}\theta. \tag{3.16}$$

A nonzero λ_1, which arises to leading order from direct hopping between neighboring d orbitals, has been included in (3.14) for completeness and also to show that such a term does not affect the results that follow. Finally, for concreteness we take the values $\beta \simeq 0.1$ eV, $\epsilon_{xz} - \epsilon_{x^2-y^2} \simeq 1.0$ eV, and $V_{pd\pi} \simeq 1.0$ eV to obtain

$$\lambda_1 \simeq 0,$$
$$\lambda_2 \simeq 100 \text{ meV } \theta. \tag{3.17}$$

B. $YBa_2Cu_3O_{6+x}$

The O ion displacement in a buckled CuO_2-Y-CuO_2 bilayer, like the tilting in $La_{2-x}Nd_xCuO_4$, results in a nonzero $t_{ij}(xz,\sigma)$ and $t_{ij}(yz,\sigma)$. Because the geometry is different [the d orbitals are not rotated, see Fig. 1(b)] the proportionality to θ of these hopping integrals from the xz and yz orbitals to the σ orbital is larger than in $La_{2-x}Nd_xCuO_4$ by a factor which we estimate to be roughly 4.8,[24] and so in this case

$$t_{i,i+\hat{x}}(xz,\sigma) \simeq 4.8\ V_{pd\pi}\theta,$$
$$t_{i,i+\hat{x}}(yz,\sigma) \simeq 0 \tag{3.18}$$

and

$$t_{i,i+\hat{y}}(xz,\sigma) \simeq 0,$$
$$t_{i,i+\hat{y}}(yz,\sigma) \simeq 4.8 V_{pd\pi}\theta \tag{3.19}$$

and the resulting $\vec{\lambda}$ vectors are

$$\vec{\lambda}^{(1)}_{i,i+\hat{x}} = (0,\lambda,0),$$
$$\vec{\lambda}^{(1)}_{i,i+\hat{y}} = -(\lambda,0,0), \tag{3.20}$$

where

$$\lambda \simeq \frac{4.8\ V_{pd\pi}\beta}{\epsilon_{xz} - \epsilon_{x^2-y^2}}\theta. \tag{3.21}$$

(We will refer to the upper and lower layers as 1 and 2, respectively.)

An important point for what follows is that because of the inversion symmetry of the unit cell of $YBa_2Cu_3O_{6+x}$ the $\vec{\lambda}_{ij}$ vectors in the lower layer are the opposite of those in the upper layer and so

$$\vec{\lambda}^{(2)}_{i,i+\hat{x}} = -(0,\lambda,0),$$
$$\vec{\lambda}^{(2)}_{i,i+\hat{y}} = (\lambda,0,0). \tag{3.22}$$

IV. MAGNETIC ANISOTROPY IN $La_{2-x}Nd_xCuO_4$

In order to derive the effective spin Hamiltonian for $La_{2-x}Nd_xCuO_4$ it is necessary to consider the large U/t limit of (3.8) with $\vec{\lambda}_{ij}$ vectors given by (3.14) when there is one electron per site. Before doing this it is useful to analyze the structure of this model by considering the motion it describes for a single electron. It is natural to decompose $\vec{\lambda}_{ij}$ into "frustrated" and "unfrustrated" components as follows:

$$\vec{\lambda}_{i,i+\hat{x}} = (-1)^{x_i+y_i}\Big\{\alpha_1(\cos\chi, \sin\chi, 0) + \alpha_2(\cos\chi, -\sin\chi, 0)\Big\}, \tag{4.1}$$

$$\vec{\lambda}_{i,i+\hat{y}} = -(-1)^{x_i+y_i}\Big\{\alpha_1(\cos\chi, \sin\chi, 0) - \alpha_2(\cos\chi, -\sin\chi, 0)\Big\}, \tag{4.2}$$

where $\alpha_1 = (\lambda_1 + \lambda_2)/2$ and $\alpha_2 = (\lambda_1 - \lambda_2)/2$. To see why this decomposition is useful consider the hopping of an electron around a single plaquette according to (3.8) for (i) $\alpha_1 = 0$, $\alpha_2 \neq 0$, and (ii) $\alpha_1 \neq 0$, $\alpha_2 = 0$. For case (i) (unfrustrated) the sign of the spin precession oscillates and no net precession occurs [Fig. 2(a)] while for case (ii) (frustrated) the sign of the precession does not oscillate and there is a net precession of $\simeq 8\alpha_1/t$ [Fig. 2(b)]. As emphasized by SEA (Ref. 8) case (i) is special: When $\alpha_2 = 0$ it is possible to perform a unitary transforma-

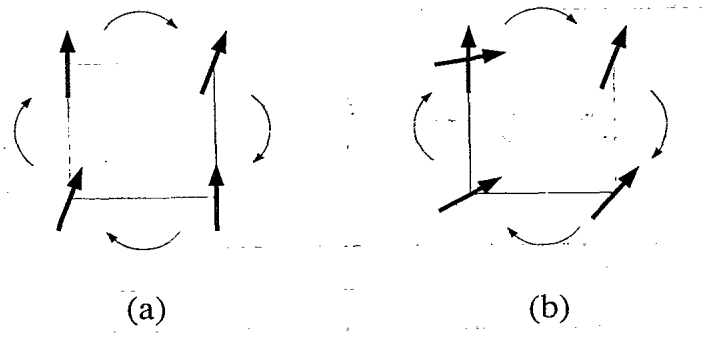

FIG. 2. (a) Unfrustrated and (b) frustrated spin precession about a single plaquette in the presence of a tilting distortion. The precession shown in (a) is unfrustrated because the electron spin returns to its original value upon hopping around any closed loop. The precession shown in (b) is frustrated because an electron which hops around a single plaquette acquires a finite spin precession. While it is always possible to eliminate the unfrustrated precession by a unitary transformation the frustrated precession cannot be so removed and thus is responsible for any physical anisotropy in spin space due to spin-orbit coupling.

tion which maps (3.8) onto a precession-free (isotropic) Hamiltonian. The nontrivial physics is thus due to the frustrated precession and it is precisely this which is described by (1.1).

The unitary transformation which eliminates the unfrustrated precession in (3.8) corresponds to a local rotation in spin space. For $\theta, \alpha_2/t \ll 1$ this unitary transformation is represented by the operator (see Appendix)

$$U = \exp\left\{ i \sum_j (-1)^{(x_j+y_j)} \frac{2\alpha_2}{t} (\cos\chi, -\sin\chi, 0) \cdot \vec{S}_j \right\} \tag{4.3}$$

under which (3.8) becomes, to leading order in α/t,

$$UHU^\dagger \simeq \sum_{\substack{\langle ij \rangle \\ \alpha\beta}} \left\{ c^\dagger_{i\alpha} \left(-t\delta_{\alpha\beta} + i\vec{\lambda}'_{ij} \cdot \vec{\sigma}_{\alpha\beta} \right) c_{j\beta} + \text{H.c.} \right\} + U \sum_i n_{i\uparrow} n_{i\downarrow}, \tag{4.4}$$

where $\vec{\lambda}'_{i,i+\hat{x}} = (-1)^{x_i+y_i}\alpha_1(\cos\chi, \sin\chi, 0)$ and $\vec{\lambda}'_{i,i+\hat{y}} = -\vec{\lambda}'_{i,i+\hat{x}}$. If a global rotation in spin space is then performed to bring the z axis parallel to $(\cos\chi, \sin\chi, 0)$ the result is (1.1) with $\phi_{i,i+\hat{x}} = (-1)^{(x_i+y_i)} 2\tan^{-1}(\alpha_1/t) \sim (-1)^{(x_i+y_i)} 0.1\theta$ and $\phi_{i,i+\hat{y}} = -\phi_{i,i+\hat{x}}$. It follows that to leading order in θ the energy spectrum of (3.8) is independent of the tilt axis angle χ and depends only on the octahedral tilt angle θ.

At half-filling and when $U \gg t$ the effective spin Hamiltonian arising from (1.1) is (up to an irrelevant constant) (Ref. 7)

$$H_{SE} = J \sum_{\langle ij \rangle} \Big\{ S^z_i S^z_j + \cos\phi_{ij} (S^x_i S^x_j + S^y_i S^y_j) + \sin\phi_{ij} (S^x_i S^y_j - S^y_i S^x_j) \Big\}. \tag{4.5}$$

The $\sin\phi_{ij} J\hat{z} \cdot (\vec{S}_i \times \vec{S}_j)$ term in (4.5) is minimized by a four sublattice state which only becomes stable when the magnitude of this term is larger than J.[15] This is never the case here and so this term is completely frustrated, there is no spin canting, and the remaining $\cos\phi_{ij}$ easy axis line the spins up along the z axis.

The classical ground state of (4.5) has no weak ferromagnetic moment and so seems to disagree with experiment. However, this is no longer true in the physical spin-space coordinate system. Once the local rotations used to transform (3.8) into (1.1) and also the global rotation which brought the z axis in spin space parallel to $(\cos\chi, \sin\chi, 0)$ are undone the spins which once were parallel to the z axis become nearly aligned along the $(\cos\chi, -\sin\chi, 0)$ direction except for a slight cant out of the CuO plane with the canting angle given by

$$\Theta_{\text{wf}} = \frac{2\alpha_2 \sin 2\chi}{t} \simeq 0.1\theta \sin 2\chi. \tag{4.6}$$

The spin configuration in the physical basis for a specific χ between 0 and $\pi/4$ is shown in Fig. 3, together with the frustrated and unfrustrated spin precession axes. In the LTO phase ($\chi = \pi/4$) (4.6) agrees with experiment: the spins point nearly parallel to the orthorhombic **c** axis and cant out of the plane through the angle $\Theta_{\text{wf}} \simeq 0.005$.[5] As χ decreases the ratio of the weak ferromagnetic moment to θ also decreases and this decrease should be experimentally observable in the *Pccn* phase of $La_{2-x}Nd_xCuO_4$.

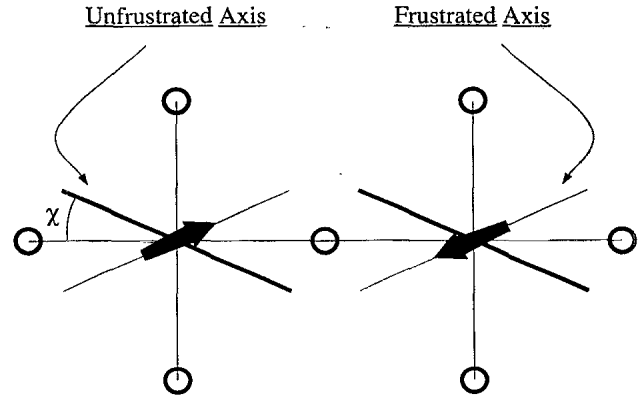

FIG. 3. Two neighboring CuO clusters in the *Pccn* phase of $La_{2-x}Nd_xCuO_4$. The heavy line is the $(\cos\chi, \sin\chi, 0)$ axis about which the CuO_6 octahedra are tilted through an angle θ. The light line is the $(\cos\chi, -\sin\chi, 0)$. The spin precession of a single electron which hops in the presence of this tilting distortion is a combination of frustrated precession about the light axis and unfrustrated precession about the heavy axis. The classical ground state of the effective spin Hamiltonian describing this system at half filling is also shown. The spins are nearly lined up along the frustrated axis except for a slight cant out of the plane by an angle which is proportional to $\sin(2\chi)$.

Given the classical ground state of (4.5) the linearized spin-wave spectrum can be calculated using standard methods.[25] The result is a twofold degenerate spectrum defined within the AFM zone with dispersion (here and throughout the paper $\vec{q}$ is in units of inverse lattice spacing),

$$\omega(\vec{q}) = 2SJ \Big[4 - \cos^2\phi(\cos q_x + \cos q_y)^2 - \sin^2\phi(\cos q_x - \cos q_y)^2 \Big]^{\frac{1}{2}}. \tag{4.7}$$

The two zone-center modes, which in the physical basis correspond to in-plane and out-of-plane spin waves, have a gap of $4SJ\sin\phi$. For the parameters used above this is $\simeq 3.0$ meV which agrees roughly with the observed zone-center spin-wave gaps of ~ 1.5 meV and ~ 2.5 meV in La_2CuO_4.[16,17] Note, however, that the theory presented here unambiguously predicts that the in-plane and out-of-plane spin-wave gaps should be equal, while experimentally these gaps have different values. It is probable that this discrepancy is due to either dipolar interactions or SO corrections to direct exchange, two sources

of anisotropic spin interactions which have not been included in this calculation.

V. MAGNETIC ANISOTROPY IN $YBa_2Cu_3O_{6+x}$

Before studying the properties of a CuO_2-Y-CuO_2 bilayer it is useful to first consider the simple toy model shown in Fig. 4: Two coupled chains in the presence of a buckling distortion. This model has the advantage of simplicity and the basic physics is similar to that of the more complex two-dimensional bilayer. The spin Hamiltonian for this system can be written

$$H^{(1D)} = H_1^{(1D)} + H_2^{(1D)} + H_{12}^{(1D)}, \tag{5.1}$$

where

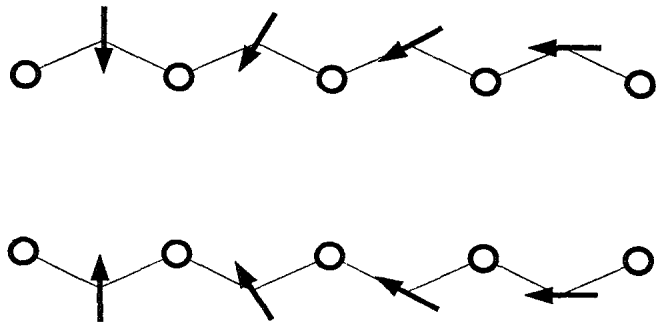

FIG. 4. Two buckled CuO "chains" representing the toy model described by (5.1). The spin configuration shown is one possible classical ground state in the absence of interchain coupling. The DM interactions induced by the buckling cause the spins to form a spiral, but because the buckling in the bottom layer is opposite to that of the top layer the spirals in the two chains have opposite senses.

$$H_1^{(1D)} = J\sum_i \left\{ S_{1,i}^x S_{1,i+1}^x + \cos\phi(S_{1,i}^y S_{1,i+1}^y + S_{1,i}^z S_{1,i+1}^z) + \sin\phi(S_{1,i}^y S_{1,i+1}^z - S_{1,i}^z S_{1,i+1}^y) \right\}, \tag{5.2}$$

$$H_2^{(1D)} = J\sum_i \left\{ S_{2,i}^x S_{2,i+1}^x + \cos\phi(S_{2,i}^y S_{2,i+1}^y + S_{2,i}^z S_{2,i+1}^z) - \sin\phi(S_{2,i}^y S_{2,i+1}^z - S_{2,i}^z S_{2,i+1}^y) \right\} \tag{5.3}$$

and where we also include an isotropic interchain coupling

$$H_{12}^{(1D)} = J_{12}\sum_i \vec{S}_{1,i}\cdot\vec{S}_{2,i}, \tag{5.4}$$

where 1D denotes one dimensional.

First consider the case $J_{12} = 0$. If we define the unitary operator

$$U_a(\phi) = \exp\left\{ i\phi \sum_i x_i S_{a,i}^x \right\}. \tag{5.5}$$

then it is possible to transform away the DM interactions in the two chains as follows:

$$U_1(\phi)H_1^{(1D)}U_1^\dagger(\phi) = J\sum_i \vec{S}_{1,i}\cdot\vec{S}_{1,i+1} \tag{5.6}$$

$$U_2(-\phi)H_2^{(1D)}U_2^\dagger(-\phi) = J\sum_i \vec{S}_{2,i}\cdot\vec{S}_{2,i+1}. \tag{5.7}$$

The eigenvalues of $H_1^{(1D)}$ and $H_2^{(1D)}$ are therefore the same as those of two uncoupled isotropic Heisenberg models. The corresponding eigenvectors are, however, different. For example, consider the classical ground-state manifold of H_1. This manifold is infinitely degenerate because (5.6), which is a unitary equivalent of $H_1^{(1D)}$, is isotropic in spin space. The ground states of $H_1^{(1D)}$, however, are not the same as the ground states of (5.6). Two extreme cases are (i) the spins lie in the yz plane and form a spiral with pitch angle ϕ, and (ii) the spins are parallel to the x axis and form a Néel state. For both cases the energy gain per site over having the spins lying uncanted in the yz plane is $JS^2\sin\phi$ and so these states are degenerate.

The system changes qualitatively when the slightest interchain coupling is introduced. Figure 4 shows one of the degenerate classical ground states of the system when $J_{12} = 0$ in which the spins spiral in the yz plane. Note that the senses of the spirals in the two chains are opposite. Any finite J_{12} will thus frustrate this spiral and the spins will prefer to point in the x direction so that J_{12} is unfrustrated. The classical ground state is then

$$\begin{aligned} \vec{S}_{1,i} &= S(1,0,0)(-1)^i, \\ \vec{S}_{2,i} &= S(1,0,0)(-1)^{i+1}. \end{aligned} \tag{5.8}$$

The linearized spin-wave spectrum about the ground state (5.8) consists of two twofold degenerate branches with dispersions

$$\omega^{(\pm)}(q) = 2SJ\left(1 + 2J_{12}/J - \cos^2\phi\cos^2 q - \sin^2\phi\sin^2 q \pm 2\cos\phi\cos q\sqrt{(J_{12}/J)^2 + \sin^2\phi\sin^2 q} \right)^{\frac{1}{2}}. \tag{5.9}$$

In Fig. 5(a) these two spin-wave dispersions are plotted for small q, $J_{12} = 0$ and $\phi = 0.02$. As expected, in this case the energy spectrum is the same as for two isotropic spin chains, the only difference being that the zeros of the spectra

have been shifted from $q = 0$ to $q = \pm\phi$ [this shift occurs because $U(\pm\phi)$ does no commuting with the translation operator]. Figure 5(b) then shows $\omega^{(-)}(q)$ for $J_{12} = 0.01J$. For these parameters the spectrum has evolved into a low-lying "acoustic" branch and a high energy "optic" branch (not shown in the figure) in which the spins in different chains precess, respectively, in and out of relative AFM phase. Note that the $q = 0$ acoustic mode has acquired a gap because of the Ising-like isotropy induced by J_{12}.

The corresponding problem for two coupled planes is somewhat more complex. The effective Hamiltonian for a single CuO_2-Y-CuO_2 bilayer is again of the form

$$H^{(2D)} = H_1^{(2D)} + H_2^{(2D)} + H_{12}^{(2D)} \tag{5.10}$$

where $H_1^{(2D)}$ describes the "upper" layer in which the in-plane O ions are buckled downwards

$$H_1^{(2D)} = J\sum_i \Big\{ S^y_{1,i}S^y_{1,i+\hat{x}} + \cos\phi(S^x_{1,i}S^x_{1,i+\hat{x}} + S^z_{1,i}S^z_{1,i+\hat{x}}) + \sin\phi(S^x_{1,i}S^z_{1,i+\hat{x}} - S^z_{1,i}S^x_{1,i+\hat{x}}) + S^x_{1,i}S^x_{1,i+\hat{y}} + \cos\phi(S^y_{1,i}S^y_{1,i+\hat{y}} + S^z_{1,i}S^z_{1,i+\hat{y}}) - \sin\phi(S^y_{1,i}S^z_{1,i+\hat{y}} - S^z_{1,i}S^y_{1,i+\hat{y}}) \Big\}, \tag{5.11}$$

$H_2^{(2D)}$ describes the "lower" layer in which the in-plane O ions are buckled upwards

$$H_2^{(2D)} = J\sum_i \Big\{ S^y_{2,i}S^y_{2,i+\hat{x}} + \cos\phi(S^x_{2,i}S^x_{2,i+\hat{x}} + S^z_{2,i}S^z_{2,i+\hat{x}}) - \sin\phi(S^x_{2,i}S^z_{2,i+\hat{x}} - S^z_{2,i}S^x_{2,i+\hat{x}}) + S^x_{2,i}S^x_{2,i+\hat{y}} + \cos\phi(S^y_{2,i}S^y_{2,i+\hat{y}} + S^z_{2,i}S^z_{2,i+\hat{y}}) + \sin\phi(S^y_{2,i}S^z_{2,i+\hat{y}} - S^z_{2,i}S^y_{2,i+\hat{y}}) \Big\}, \tag{5.12}$$

and we again assume that the layers are coupled by

$$H_{12}^{(2D)} = J_{12}\sum_i \vec{S}_{1,i}\cdot\vec{S}_{2,i}. \tag{5.13}$$

The Hamiltonians (5.11) and (5.12) are obtained as before by taking the large U/t limit of (3.8) with $\vec{\lambda}_{ij}$ vectors given by (3.20) and (3.22). A similar Hamiltonian (without the $\cos\phi$ terms) was derived by Coffey, Rice, and Zhang[11] for a single CuO layer in $YBa_2Cu_3O_{6+x}$. These authors noted that the classical ground state of a single layer is not a (possibly canted) Néel state. Instead, because the ϕ_{ij}'s do not alternate in sign as they do in $La_{2-x}Nd_xCuO_4$, the spins want to form a spiral.[11,15] It is interesting to note that the problem of finding the classical ground state of (5.10) is nontrivial because bonds which point in the x direction favor spiraling about the y axis, while bonds which point in the y direction favor spiraling about the x axis and there is no classical ground state which spirals in this way. Fortunately, any difficulties associated with finding the classical ground state of (5.11) are probably irrelevant; just as the coupled chains discussed above the spiral tendencies in the two layers are opposed to one another and so interlayer exchange, if sufficiently strong, will lock in a commensurate AFM state.

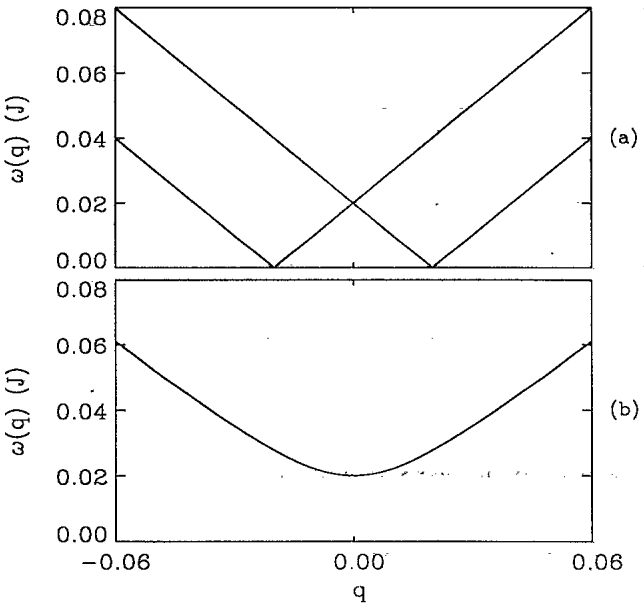

FIG. 5. Spin-wave spectrum for two buckled chains when (a) $J_{12} = 0$ and (b) $J_{12} = 0.01J$. In (a) the spin-wave spectrum is identical to that of two isotropic Heisenberg models except that q has been shifted by $\pm\phi$. In (b) there is a finite interlayer coupling and the system has acquired an Ising-like character and a gap.

Consider the set of classical Néel state parametrized as

$$\vec{S}_{1,i} = S(\cos\gamma\cos\eta, \sin\gamma\cos\eta, \sin\eta)(-1)^{(x_i+y_i)},$$
$$\vec{S}_{2,i} = S(\cos\gamma\cos\eta, \sin\gamma\cos\eta, \sin\eta)(-1)^{(x_i+y_i+1)}. \tag{5.14}$$

Treating these as variational states for (5.10) yields an energy per site of

$$E[\phi,\eta] = -JS^2[\cos\phi(\sin^2\eta + 1) + \cos^2\eta] - J_{12}S^2 \tag{5.15}$$

which is minimized when $\eta = 0$. Thus the lowest energy Néel states are those in which the spins lie in the xy plane. The origin of this easy plane is rather subtle. It arises from the $\cos\phi_{ij}$ easy-axis terms in (5.10). These terms favor spins parallel to the x direction on bonds which point in the y direction, and *vice versa*, so that

when a classical Néel state is rotated in the plane the energy gain on one type of bond increases while that on the other type decreases in such a way that the total energy remains constant.

The classical spin-wave spectrum about (5.14) when $\nu = 0$ can again be calculated using standard methods. The resulting spectrum has four branches with dispersions given by

$$\omega_a^{(\pm)}(\vec{q}) = 2JS\Big[[A(0) + 2J_{12}/J]A(0) - A(q)B(\vec{q}) - C(\vec{q})^2 \pm (\{A(0)B(\vec{q}) - [A(0) + 2J_{12}/J]A(\vec{q})\}^2 + 4C(\vec{q})^2 A(\vec{q})B(\vec{q}))^{\frac{1}{2}}\Big]^{\frac{1}{2}}, \tag{5.16}$$

$$\omega_b^{(\pm)}(\vec{q}) = 2JS\Big[[A(0) + 2J_{12}/J]A(0) - A(\vec{q})B(\vec{q}) - C(\vec{q})^2 \pm (\{[A(0) + 2J_{12}/J]B(\vec{q}) - A(0)A(\vec{q})\}^2 + 4C(\vec{q})^2 A(\vec{q})B(\vec{q}))^{\frac{1}{2}}\Big]^{\frac{1}{2}}, \tag{5.17}$$

where

$$A(\vec{q}) = (\cos^2\gamma + \sin^2\gamma\cos\phi)\cos q_x + (\sin^2\gamma + \cos^2\gamma\cos\phi)\cos q_y, \tag{5.18}$$

$$B(\vec{q}) = \cos\phi(\cos q_x + \cos q_y), \tag{5.19}$$

$$C(\vec{q}) = \sin\phi(\sin\gamma\sin q_x + \cos\gamma\sin q_y). \tag{5.20}$$

It can now be made apparent that the Néel state (5.14) with $\eta = 0$ is not stable for small J_{12}/J. In the limit $q_x, q_y, \phi \ll 1$, $J_{12}/J \lesssim \phi^2$, and $\gamma = 0$ the dispersion of the lowest lying branch is well approximated by

$$\omega_a^{(-)}(\vec{q}) \simeq 2JS\left[\left(\frac{8J_{12} - 6J\phi^2}{4J_{12} + J\phi^2}\right)q_x^2 + 2q_y^2\right]^{\frac{1}{2}}. \tag{5.21}$$

When $J_{12}/J < 3\phi^2/4$ the frequencies of this branch become complex for a region in q space near $\vec{q} = 0$. These complex frequencies signal the appearance of unstable modes which grow exponentially with time.

In Fig. 6 the spin-wave dispersions given by (5.17) and (5.20) are shown for $\gamma = 0$, $q_y = 0$ and q_x small when $\phi = 0.02$ and $J_{12}/J = 0.0$, $\phi^2/2$, $3\phi^2/4$ and 0.01. The hatched regions denote q values for which the spin-wave frequencies become complex indicating that the Néel state is unstable. As J_{12} is increased the spin-wave spectrum evolves in the following way. First, for $J_{12} = 0.0$ there are two twofold degenerate branches, the lower two of which become complex at small q_x. Then, as J_{12}/J is gradually increased the degenerate branches split and the region of instability in q space shrinks so that when $J_{12}/J \simeq \phi^2/2$ there is only one unstable branch ($\omega_a^{(-)}$) and when $J_{12}/J \simeq 3\phi^2/4$ the complex frequencies disappear entirely from the spectrum and the Néel state becomes locally, and almost certainly globally, stable.

For the physically relevant case $J \gg J_{12} \gg \phi^2 J$ the dispersion of the four spin-wave branches are approximately given by

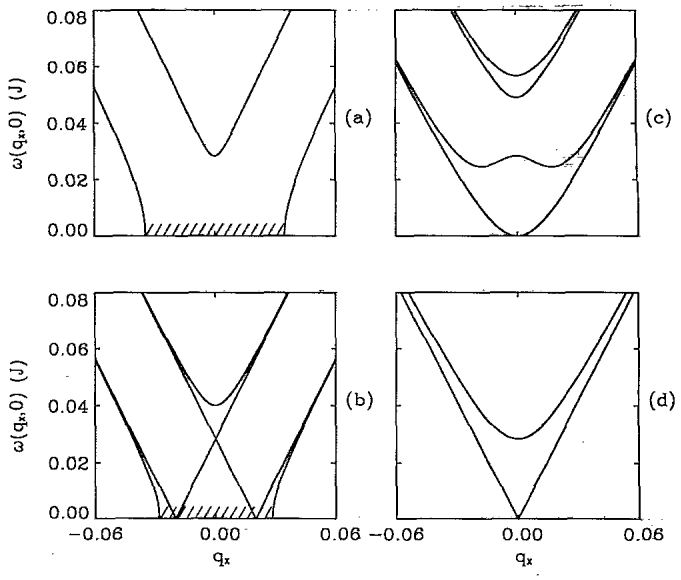

FIG. 6. Spin-wave spectrum about a Néel state with spins parallel to the x direction for a CuO_2-Y-CuO_2 bilayer in $YBa_2Cu_3O_{6+x}$ for J_{12}/J equal to (a) 0; (b) 0.25ϕ; (c) 0.75ϕ; and (d) 0.01 where $\phi \simeq 0.02$. The hatched regions represent q values where one or more of the frequencies are complex indicating an instability. There are four modes which degenerate into two when (a) $J_{12}/J = 0$. As J_{12}/J increases these modes split. In (b) one of the two unstable modes has become stable. In (c) both have become stable and in (d) the two higher-lying optic modes are not shown and the two lowest modes correspond to a gapless in-plane and a gapped out-of-plane mode in agreement with experiment.

$$\omega_a^{(-)}(\vec{q}) \simeq 2\sqrt{2}JS|\vec{q}|, \quad (5.22)$$

$$\omega_b^{(-)}(\vec{q}) \simeq 2\sqrt{2}JS\sqrt{\phi^2 + |\vec{q}|^2}, \quad (5.23)$$

$$\omega_a^{(+)}(\vec{q}) \simeq \omega_b^{(+)}(\vec{q}) \simeq 2JS\sqrt{8J_{12}/J + |\vec{q}|^2}. \quad (5.24)$$

Such a spin-wave spectrum is precisely what is expected for a bilayer made up of two easy-plane antiferromagnets.[20] In this limit $\omega_a^{(-)}(\vec{q})$ and $\omega_b^{(-)}(\vec{q})$ have evolved into low-energy modes corresponding to gapless in-plane and gapped out-of-plane spin-waves, respectively. These modes are acoustic modes in the sense defined above: the spins in the two layers precess in relative AFM phase with one another. Figure 6(d) shows these low-lying modes for $J_{12}/J \simeq 0.01$. The out-of-plane mode has a gap of $2\sqrt{2}SJ\phi$ a result which is consistent with the experimental observation of a gapped out-of-plane zone-center mode.[6] The remaining branches $\omega_a^{(+)}(\vec{q})$ and $\omega_b^{(+)}(\vec{q})$ have evolved into the high-energy optic modes in which spins in the two layers precess out of AFM phase and have a gap of $4\sqrt{2}S\sqrt{J_{12}J}$. These modes have not been seen experimentally for energies up to ~ 50 meV (Ref. 6) indicating that $J_{12} > 0.01J$. The interlayer coupling is therefore large enough to lock in the Néel state according to the above scenario.

VI. CONCLUSIONS

In this paper the anisotropic corrections to superexchange arising from SO coupling in the distorted CuO layers in $La_{2-x}Nd_xCuO_4$ (tilting distortion) and $YBa_2Cu_3O_{6+x}$ (buckling distortion) have been calculated using Moriya's method.[1] Special care has been taken to include the higher-order symmetric anisotropy terms whose importance has recently been emphasized by SEA.[8]

In the $La_{2-x}Nd_xCuO_4$ system in the presence of a tilting distortion it was shown that regardless of the tilt axis it is always possible to find a local coordinate system in spin space in which the SO-induced spin precession of moving electrons has the same form. This form is precisely that which was studied in Ref. 7 and is described by Hamiltonian (1.1). In this special spin-space coordinate system the classical ground state of the effective spin Hamiltonian has no weak ferromagnetic moment but when the system is viewed in the physical coordinate system a weak ferromagnetic moment appears. The ratio of the octahedral tilt angle to the weak ferromagnetic moment depends on the tilt axis according to (4.6) and so it decreases as the tilt axis moves from $\langle 110 \rangle$ in the LTO phase to $\langle 100 \rangle$ in a hypothetical insulating AFM LTT material. The experimental observation of the reduction of this ratio in the *Pccn* phase of $La_{2-x}Nd_xCuO_4$ would provide a test of the theory discussed here and in Ref. 8. One unresolved problem with the theory is that it predicts that regardless of the tilt axis there should be only *one* spin-wave gap—a prediction which is at odds with the experimental observation of two different gaps for the in-plane and out-of-plane zone-center modes. It is likely that this discrepancy is due to the additional anisotropy caused either by dipolar interactions or SO corrections to direct exchange. However, a full treatment of the problem including these interactions has not yet been carried out.

When the same method for calculating the SO corrections to superexchange in $La_{2-x}Nd_xCuO_4$ is applied to the buckled CuO_2-Y-CuO_2 bilayers in $YBa_2Cu_3O_{6+x}$ the resulting Hamiltonian is quite different from what has been used previously to model this system. The Hamiltonian obtained here describes a system in which the spins in each individual CuO layer tend to form a spiral pattern. However, one consequence of the inversion symmetry of the unit cell of $YBa_2Cu_3O_{6+x}$ is that the senses of the spirals favored by the two CuO planes in a given bilayer are opposed to one another. When a weak interlayer coupling is included the spiraling becomes frustrated and a commensurate AFM state is stabilized. For physical parameters the low-energy spin-wave spectrum agrees with what is seen experimentally: there is an in-plane acoustic mode and an out-of-plane gapped mode.

We conclude on a speculative note. In Ref. 7 it was argued that the frustrated DM terms in La_2CuO_4 can give rise to physics away from half-filling. In particular, doped holes can gain energy from their s.o.-induced spin precession as they move through a commensurate spin background. This energy gain is similar to that which occurs when holes move through a spiral state.[7] We have shown here that frustrated DM terms are present in $YBa_2Cu_3O_{6+x}$, and the size of these terms is significantly larger than in La_2CuO_4 (by roughly a factor of 5). Because of this, holes doped into a CuO_2-Y-CuO_2 bilayer can also gain energy through their spin precession. In this case the maximum energy gain occurs when the spins form a commensurate Néel background and are lined up parallel to the z direction. When moving through such a spin background doped holes see, effectively, a so-called "double spiral."[26] We note that a strong tendency for commensurate spin fluctuations in superconducting $YBa_2Cu_3O_{6+x}$ has been observed in both NMR (Ref. 27) and neutron-scattering[6,21] experiments while in doped La_2CuO_4 spin fluctuations appear to be incommensurate.[28,29] It is tempting to speculate that SO effects such as those discussed here and in (Ref. 7) may play some role in determining the different spin dynamics of these two systems.

ACKNOWLEDGMENTS

The author acknowledges useful discussions with A. Aharony, D. Arovas, J. Axe, R. Hlubina, T.M. Rice, H. Viertiö, and F.C. Zhang. This work was supported by a grant from the Swiss National Fund.

APPENDIX

In this appendix the exact unitary transformation which maps Hamiltonian (3.8) into (1.1) is constructed for arbitrary χ and θ. This transformation is most easily represented as a sequence of two local rotations in spin space.

The first rotation eliminates the component of the unfrustrated precession perpendicular to the frustrated axis and is generated by

$$U^{(1)} = \exp\left\{ i \sum_j (-1)^{(x_j+y_j)} 2 \tan^{-1}\left(\frac{\alpha_2 \sin 2\chi}{t}\right) (\cos\chi, -\sin\chi, 0) \cdot \vec{S}_j \right\}. \tag{A1}$$

When $U^{(1)}$ is applied to Hamiltonian (3.8) the result is

$$U^{(1)} H U^{(1)\dagger} = H' = \sum_{\substack{\langle ij \rangle \\ \alpha\beta}} \left\{ c^\dagger_{i\alpha} \left[\sqrt{t^2 + (\alpha_2 \sin 2\chi)^2}\, \delta_{\alpha\beta} + i \vec{\lambda}'_{ij} \cdot \vec{\sigma}_{\alpha\beta} \right] c_{j\beta} + \text{H.c.} \right\} + U \sum_i n_{i\uparrow} n_{i\downarrow}, \tag{A2}$$

where the transformed $\vec{\lambda}'$ vectors are

$$\begin{aligned} \vec{\lambda}'_{i,i+\hat{x}} &= (-1)^{x_i+y_i} (\alpha_1 - \alpha_2 \cos 2\chi)(\cos\chi, \sin\chi, 0), \\ \vec{\lambda}'_{i,i+\hat{y}} &= -(-1)^{x_i+y_i} (\alpha_1 + \alpha_2 \cos 2\chi)(\cos\chi, \sin\chi, 0). \end{aligned} \tag{A3}$$

The precession axes on all the links in the lattice are now parallel to one another. A further rotation generated by

$$U^{(2)} = \exp\left\{ i \sum_j (-1)^{(x_j+y_j)} 2 \tan^{-1}\left(\frac{\alpha_2 \cos 2\chi}{\sqrt{t^2 + \alpha_2^2 \sin^2 2\chi}} \right) (\cos\chi, \sin\chi, 0) \cdot \vec{S}_j \right\} \tag{A4}$$

then ensures that the precession has the same magnitude on all the links. Upon applying this transformation the Hamiltonian becomes

$$U^{(2)} H' U^{(2)\dagger} = \sum_{\substack{\langle ij \rangle \\ \alpha\beta}} \left\{ c^\dagger_{i\alpha} \left(\xi_{ij} \delta_{\alpha\beta} + i \vec{\lambda}''_{ij} \cdot \vec{\sigma}_{\alpha\beta} \right) c_{j\beta} + \text{H.c.} \right\} + U \sum_i n_{i\uparrow} n_{j\downarrow}, \tag{A5}$$

where $\xi_{i,i+\hat{x}} = \sqrt{t^2 + \alpha_2^2 + \alpha_1\alpha_2 \sin 2\chi}$, $\xi_{i,i+\hat{y}} = \sqrt{t^2 + \alpha_2^2 - \alpha_1\alpha_2 \sin 2\chi}$; and

$$\vec{\lambda}''_{i,i+\hat{x}} = (-1)^{x_i+y_i} \alpha_1 (\cos\chi, \sin\chi, 0) \tag{A6}$$

$$\vec{\lambda}''_{i,i+\hat{y}} = -\vec{\lambda}''_{i,i+\hat{x}}. \tag{A7}$$

If the second order in θ corrections to the direct hopping integral are ignored ($\xi_{ij} \simeq t$) and a global rotation in spin space is performed so that the z axis is parallel to $(\cos\chi, \sin\chi, 0)$ the result is Hamiltonian (1.1) with $(-1)^{(x_i+y_i)} 2 \tan^{-1}(\alpha_1/t) \sim (-1)^{(x_i+y_i)} 0.1\theta$ and $\phi_{i,i+\hat{y}} = -\phi_{i,i+\hat{x}}$.

[1] T. Moriya, Phys. Rev. **120**, 91 (1960).
[2] P.W. Anderson, Phys. Rev. **115**, 2 (1959).
[3] I. Dzyaloshinski, J. Phys. Chem. Solids **4**, 241 (1958).
[4] In this paper all corrections to superexchange due to SO coupling will be referred to as DM interactions. This includes (using the notation of Ref. 1) antisymmetric terms of the form $\mathbf{D} \cdot (\mathbf{S} \times \mathbf{S})$ which are linear in SO coupling, and symmetric terms of the form $\mathbf{S} \cdot \mathbf{\Gamma} \cdot \mathbf{S}$ which are quadratic.
[5] T. Thio *et al.*, Phys. Rev. B **38**, 905 (1988).
[6] J. Rossat-Mignod *et al.*, Physica B **169**, 58 (1991), and references therein.
[7] N.E. Bonesteel, T.M. Rice, and F.C. Zhang, Phys. Rev. Lett. **68**, 2684 (1992).
[8] L. Shekhtman, O. Entin-Wohlman, and A. Aharony (unpublished); L. Shekhtman, A. Aharony, and O. Entin-Wohlman (unpublished).
[9] M. Crawford *et al.*, Phys. Rev. B **44**, 7749 (1991).
[10] B. Büchner *et al.*, Physica C **185–189**, 903 (1991).
[11] D. Coffey, T.M. Rice, and F.C. Zhang, Phys. Rev. B **44**, 10 112 (1991).
[12] J.F. Bringley, S.S. Trail, and B.A. Scott, J. Solid State Chem. **86**, 310 (1990).
[13] J.D. Axe *et al.*, Phys. Rev. Lett. **62**, 2751 (1989).
[14] S. Chakravarty, in *High-Temperature Superconductivity*, edited by K.S. Bedell *et al.* (Addison-Wesley, Reading, MA, 1990); E. Manousakis, Rev. Mod. Phys. **63**, 1 (1991), and references therein.
[15] D. Coffey, K. Bedell, and S.A. Trugman, Phys. Rev. B **42**, 6509 (1990).
[16] C.J. Peters *et al.*, Phys. Rev. B **37**, 9761 (1988).
[17] R.T. Collins *et al.*, Phys. Rev. B **37** (1988).
[18] W. Koshibae, Y. Ohta, and S. Maekawa (unpublished).
[19] J.S. Swinnea and H. Steinfink, J. Matter Res. **2**, 424 (1987).
[20] See, for example, H. Alloul, in *High Temperature Superconductivity*, Proceedings of the Thirty-Ninth Scottish Universities Summer School in Physics, edited by D.P. Mc Tunstall and W. Barford (Hilgar, Bristol, 1992), and references therein.
[21] J.M. Tranquada, P.M. Gehring, G. Shirane, S. Shamoto, and M. Sato, Phys. Rev. B **46**, 5561 (1992).
[22] V.J. Emery and G. Reiter, Phys. Rev. B **38**, 4547 (1988).
[23] See, for example, J.C. Slater, *Quantum Theory of Matter* (McGraw-Hill, New York, 1968), pp. 306–309.
[24] See, for example, W. A. Harrison, *Electronic Structure and*

the Properties of Solids (Freeman, San Francisco, 1980).
[25]F. Keffer, in *Handbuch der Physik*, edited by S. Flügge (Springer-Verlag, Berlin, 1966), Vol. 18, Pt. 2, p. 1.
[26]C.L. Kane *et al.*, Phys. Rev. B **41**, 2653 (1990).
[27]R.E. Walstedt and J.W.W. Warren, Science **248**, 1082 (1990), and references therein.
[28]S-W. Cheong *et al.*, Phys. Rev. Lett. **67**, 1791 (1992); T.E. Mason, G. Aeppli, and H.A. Mook, *ibid.* **68**, 1414 (1992).
[29]P.C. Hammel, E.T. Ahrens, A.P. Reyes, P.C. Canfield, Z. Fisk, J.D. Thompson, and J.E. Schirber (unpublished).